




Prediction and Analysis of Lake Ice Phenology Dynamics Under Future Climate Scenarios Across the Inner Tibetan Plateau

Yongjian Ruan¹ , Xinchang Zhang^{2,3}, Qinchuan Xin^{1,4} , Yubao Qiu⁵ , and Ying Sun¹ **Key Points:**

- The pace of lake ice phenology change showed quite different characteristics across six sub-basins in the inner TP
- Advances in break-up end date and delays in freeze-up start date result in shortened ice duration under RCP4.5/6.0/8.5
- Inter-annual variation of lake ice phenology increases with increasing CO₂ concentration in the air

Supporting Information:

- Supporting Information S1

Correspondence to:Y. Sun,
sunying23@mail.sysu.edu.cn**Citation:**

Ruan, Y., Zhang, X., Xin, Q., Qiu, Y., & Sun, Y. (2020). Prediction and analysis of lake ice phenology dynamics under future climate scenarios across the inner Tibetan Plateau. *Journal of Geophysical Research: Atmospheres*, 125, e2020JD033082. <https://doi.org/10.1029/2020JD033082>

Received 11 MAY 2020

Accepted 7 NOV 2020

Accepted article online 12 NOV 2020

¹School of Geography and Planning, Sun Yat-Sen University, Guangzhou, China, ²School of Geography and Remote Sensing, Guangzhou University, Guangzhou, China, ³The College of Environment and Planning of Henan University, Henan University, Kaifeng, China, ⁴State Key Laboratory of Desert and Oasis Ecology, Research Center for Ecology and Environment of Central Asia, Chinese Academy of Sciences, Urumqi, China, ⁵Key Laboratory of Digital Earth Science, Aerospace Information Research Institute, Chinese Academy of Sciences, Beijing, China

Abstract How climate change influences lake ice phenology is important in understanding the climate-lake interactions. This study investigates the response of lake ice phenology to future climate scenarios. Thirty-five lakes in the Tibetan Plateau were studied. Firstly, we applied a random forest (RF) model to simulate lake ice condition under different representative concentration pathways (RCPs). The results of the virtual experiments show that lake ice freeze-up start date (FUSD) and break-up end date (BUED) are well simulated by the RF model, with $R^2_{FUSD} > 0.91$ under different RCPs, and $R^2_{BUED} > 0.84$, except in RCP2.6 ($R^2 = 0.74$). Secondly, two non-parametric methods (Mann-Kendall and Sen's slope estimator) were used for analyzing the trends in lake ice phenology and its response to various emission scenarios. Lake ice phenology was largely affected by temperature changes under different RCPs, and it had a larger inter-annual variability in the early period (2002–2050) than in the later period (2050–2099). FUSD of 35 lakes delayed by an average of 0.01, 0.04, and 0.04 days/yr from 2002 to 2098 under RCP4.5, RCP6.0, and RCP8.5, whereas BUED advanced by an average of 0.04, 0.11, and 0.21 days/yr from 2003 to 2099. Both delays in FUSD and advances in BUED contributed to shortened average ice duration of 35 lakes, which shortened by 0.05, 0.14, and 0.25 days/yr from 2002 to 2098 under RCP4.5, RCP6.0, and RCP8.5, respectively. These findings could help to tackle the impacts of climate change on the lake systems.

Plain Language Summary The impacts of future climate scenarios on lake ice phenology is important in understanding the climate-lake interactions. Thirty-five lakes in the Tibetan Plateau were studied. We employed a random forest (RF) model to simulate lake ice condition under different representative concentration pathways (RCPs). The results of the virtual experiments show that lake ice freeze-up start date (FUSD) and break-up end date (BUED) are well simulated by the RF model, under different RCPs. FUSD of 35 lakes delayed by an average of 0.01, 0.04, and 0.04 days/yr from 2002 to 2098 under RCP4.5, RCP6.0, and RCP8.5, whereas BUED advanced by an average of 0.04, 0.11, and 0.21 days/yr from 2003 to 2099. Both delays in FUSD and advances in BUED contributed to shortened average ice duration of 35 lakes, which shortened by 0.05, 0.14, and 0.25 days/yr from 2003 to 2098 under RCP4.5, RCP6.0, and RCP8.5, respectively. Our results could help to tackle the impacts of climate change on the lake systems.

1. Introduction

The fifth assessment report of the Intergovernmental Panel on Climate Change (IPCC) documented a warming of the earth's climate system (Hartmann et al., 2013; Parry et al., 2007; Rosenzweig et al., 2008). Climate change has triggered changes in the earth's biological and physical systems, which has obviously affected lake systems (Rosenzweig et al., 2008; Sharma et al., 2019; Sorvari et al., 2002). A study of 235 lakes across the world reported that lake surface temperatures rose with a mean trend of 0.34°C decade⁻¹ in summer (between 1985 and 2009), higher than that of ocean surface temperatures (0.12°C decade⁻¹) and air temperatures (0.25°C decade⁻¹) (O'Reilly et al., 2015). The lake ice cover will turn to be intermittent when the local mean air temperatures exceeded 8.4°C (Sharma et al., 2019). In the Northern Hemisphere, 14,800 lakes currently experience intermittent winter ice cover, and it has

impacted over 394 million people living (Sharma et al., 2019). In addition, warming will shorten the ice cover duration and increase the probability of carbon combustion to form greenhouse gases, thus exacerbating the greenhouse effect (O'Reilly et al., 2015).

Lake ice phenology, characterized by the timing of lake ice freezing and breaking, has changed dynamically under a changing climate and has received considerable attention (Riahi et al., 2007; van Vuuren et al., 2007; Wise et al., 2009). The study of lake ice phenology can even be traced back to 1845 (Benson et al., 2000). In the early years, lake ice phenology was often monitored by ground monitoring sites. Due to the difficult living environment, lake ground observation sites at the Tibetan Plateau (TP) are rare. With the development of satellite technology, remotely sensed images offer an alternative way for lake ice monitoring. Optical remote sensing images provide a rich data source for the lake ice studies and thus have been widely used. Kropacek et al. (2013) used the Moderate Resolution Imaging Spectroradiometer (MODIS) optical product (MYD10A2 8-day cloudless product) to obtain the lake ice condition of 59 lakes in the TP and to monitor lake ice phenology changes. Yao et al. (2016) monitored the lake ice phenology (2000–2011) of 22 lakes in the Hoh Xil region by using MODIS data products (MOD09GA). Based on MOD10A1 (Terra) and MYD10A1 (Aqua), Cai et al. (2019) monitored the lake ice phenology of 58 lakes in the TP via the open water pixels.

Considering the spatial and temporal resolution, optical remote sensing images such as MODIS and AVHRR are suitable for the monitoring of lake ice condition. However, clouds often appear in areas where atmospheric convection is active, affecting the effective detection of ground information by optical sensors (Zhang et al., 2016). As passive microwave is able to penetrate the clouds, passive microwave sensors could provide meaningful observations even under the constraints of weather conditions. Although data from passive microwave sensors have low spatial resolution, they are widely used for the monitoring of lake ice phenology in the literature. The Special Sensor Microwave/Imager (SSM/I), the Advanced Microwave Scanning Radiometer for EOS (AMSR-E), and the Advanced Microwave Scanning Radiometer 2 (AMSR2) were used for Qinghai (Cai et al., 2017; Che et al., 2009) and Nam Co (Ke et al., 2013) lake ice monitoring in the TP. Du and Kimball (2018) developed a data set named Daily Lake Ice Phenology Time Series, which was derived from the passive microwave sensors AMSR-E and AMSR2 (2002–2015). This satellite-based data set also covers the Northern Hemisphere and can provide daily lake ice condition with a spatial resolution of 5 km, but there were only a few lakes monitored by this data set in the TP. Qiu et al. (2017) conducted pixel unmixing for passive microwave images to obtain sub-pixel information of lakes. Based on it, they obtained the lake ice condition in 51 lakes across the TP. Overall, these studies mainly focused on the monitoring of lake ice phenology and corresponding data set production.

Lake ice phenology is recognized as a robust indicator of climate change (Cai et al., 2019). The prediction of change in lake ice phenology can, in turn, provide better evaluation of potential influence factors. Few studies have investigated the impact of future climatic change on lake ice phenology. Yao et al. (2013) made use of linear regression and lake dynamics models to investigate the influence of climate factors on the ice phenology of Dickie Lake (located in south-central Ontario, Canada), and the modeling approaches were then used for predicting future ice cover. Crossman et al. (2016) established the relationships among climate drivers, lake morphology, and lake physical changes via generalized linear modeling (GLM), and quantified the ice phenology changes of 72 lakes under future climate scenarios. Hewitt et al. (2018) developed multiple linear regression models to investigate the lake ice phenology changes of nine lakes across North America under different climate change scenarios. Sharma et al. (2019) employed in situ records of 513 lakes to evaluate the loss of lake ice in future climate change over the Northern Hemisphere.

The TP, which is known as the “third pole” of the earth, is the water source of several rivers and is an important reservoir of water vapor energy exchange (Kang et al., 2010; Yao et al., 2012). TP is an area with the highest concentration of high-altitude lakes (Qiao et al., 2019; Zhang, Yao, Xie, Zhang, et al., 2014; Zhang et al., 2019) and the most sensitive region influenced by global climate change, which is an ideal research area for lake ice phenology (Cai et al., 2019; Che et al., 2009; Gou et al., 2017; Kropacek et al., 2013; Liu et al., 2018; Qiu et al., 2018; Yao et al., 2016). Investigating the response of lake ice phenology to climate change in the TP is a key part of global climate change studies. Some lakes in the TP are experiencing a temperature rise which is the same as the lakes in other region of the Northern Hemisphere (Sharma et al., 2019).

Zhang, Yao, Xie, Qin, et al. (2014) analyzed 52 lakes of TP and found that the surface temperature of these lakes have exhibited an average changing rate of $0.012 \pm 0.033^{\circ}\text{C}/\text{yr}$ from 2001 to 2012. Wan et al. (2018) explored surface water temperature of 374 lakes of TP from 2001 to 2015 and found an average changing rate of $0.037^{\circ}\text{C}/\text{yr}$ of the studied lakes. Accordingly, the lake ice phenology in the TP were affected by climate change. Sharma et al. (2019) investigated the loss of lake ice based on 513 in situ records of lakes in the Northern Hemisphere, but the analysis only include one lake, i.e., the Qinghai Lake, from the TP. Overall, there is a need to investigate the interactions between future climate and lake ice phenology in the TP region.

In this paper, we aim to explore ways to predict the future lake ice phenology of the inner TP, as it may result in a significant influence owing to the feedbacks between lakes and the climate. To achieve this goal, we (1) studied 35 lakes in the inner basin of the TP; (2) used the random forest regression algorithm (Breiman, 2001) to model the lake ice condition such as FUSD and BUED based on independent variables, including climate factors and lake attributes; (3) derived the lake ice phenology dates from satellite remote sensing images for model training and validation, and made predictions using the climate data from the representative concentration pathway (RCP) data set; and (4) used the Mann-Kendall (MK) and Sen's slope estimator to analyze the variation tendency of lake ice phenology.

2. Materials

2.1. Lake Ice Phenology Data Set

We used a lake ice phenology data set (a data set of microwave brightness temperature and freeze-thaw for medium-to-large lakes over the High Asia region from 2002 to 2016) released by our previous study (Qiu et al., 2017), which is available online (<http://www.csdata.org/en/p/105/>). The data set includes a time series of lake ice condition of 51 lakes in the High Asia region (including the TP) from 2002 to 2016. It is derived from satellite observation by AMSR-E and AMSR2 with 18.7V GHz. The dynamic decomposition of passive microwave pixels method (Qiu et al., 2017) was used to estimate the brightness temperature of the lake. The processed brightness temperature curves were then used to determine the lake ice condition, such as lake ice freeze-up start date (FUSD), freeze-up end date (FUED), break-up start date (BUSD), and break-up end date (BUED). In addition, ice duration (ID) is available as calculated via BUED minus FUSD. Data for Dagze Co, Kusai Lake, and Hoh Xil Lake, which have different sizes and are located in different parts of the TP, were used for validation. The lake ice condition of these three lakes were derived from cloudless MODIS snow products compared with the processed brightness temperature curves, showing high correlation coefficients in freezing and thawing times (0.968 and 0.968, respectively). The data set has also been used in other researches, such as studying the impact of the winter North Atlantic Oscillation on the break-up date of lake ice (Liu et al., 2018); validating the MODIS-based lake ice extent and coverage data set (Qiu et al., 2019); and studying the impact of the preceding spring Antarctic Oscillation on the variations of lake ice phenology (Liu et al., 2020).

The inner TP is less affected by human activities than the other plateau areas, and it can well reflect the impact of climate change on lake ice phenology under different scenarios. The lake ice phenology data set records the lake ice phenology of 38 lakes in the inner TP, in which there are three lakes with missing data in some years. We used data from 35 major lakes in the lake ice phenology data set in our study (Figure 1). The lakes are widely located in the six sub-basins. In watershed Inner A, 10 lakes named Bamco, Dagze Co, Dung Co, Kyebxang Co, Nam Co, Ngangze Co, Norma Co, Pung Co, Selin Co, and Zige Tangco were selected; in watershed Inner B, only one lake was chosen (Zhari Namco); in watershed Inner C, two lakes, i.e., Ngangla Ringco and Rinqin Xubco, were selected; in Inner D, two lakes were chosen (Aqqikkol Lake and Ayakkum Lake); 11 lakes in Inner E were selected (Dogaicoring Qangco, Hoh Xil Lake, Kusai Lake, Lexiewudan Co, Margai Caka, Rola Co, Wulanwula Lake, Xiangyang Lake, Yanghu Lake, Yuye Lake, and Zhuonai Lake); and nine lakes were selected in the largest Inner F (Aksayqin Hu, Bairab Co, Chibzhang Co, Dorsoidong Co, Dulishi Lake, Heishi North Lake, Lumajiangdong Co, Luotuo Lake, and Memar Co). The detailed lake characteristics are shown in Table S1.

2.2. The Surface Temperature Products of RCPs

The IPCC uses emissions and climate scenarios as an important component for the better evaluation of climate change effects (Moss et al., 2010). The RCP data set is a set of specific emission scenarios presented by the IPCC (Moss et al., 2010), in which four RCP scenarios (RCP2.6/4.5/6.0/8.5) are included and each

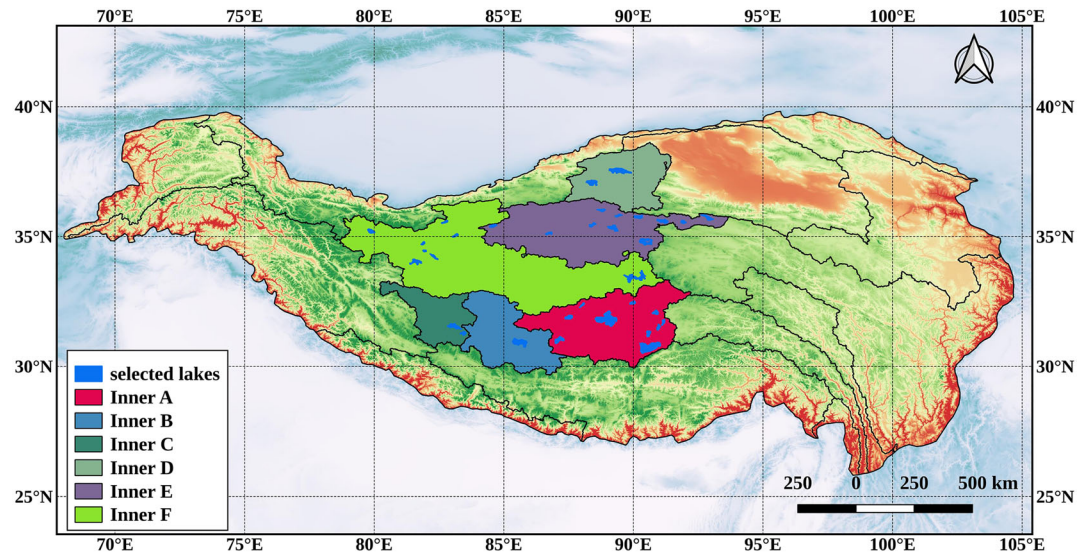


Figure 1. Spatial distribution of the 35 studied lakes over the watershed of the inner Tibetan Plateau. The name of six sub-basins were displaying in the Figure 1, and we followed the naming of six sub-basins in the study of Zhang et al. (2013) and Wan et al. (2016).

corresponds to a radiative forcing pathway (Riahi et al., 2007; van Vuuren et al., 2007; Wise et al., 2009). RCP2.6 (van Vuuren et al., 2011) is the scenario with the lowest greenhouse gas concentration level, in which atmospheric carbon dioxide concentrations peak at ~490 ppm (before 2100 and then declines). RCP4.5 (Thomson et al., 2011) and RCP6.0 (Masui et al., 2011) are stabilization scenarios with atmospheric carbon dioxide peaks at ~650 ppm and ~850 ppm (at stabilization after 2100), respectively. RCP8.5 (Riahi et al., 2011) is the scenario with the highest greenhouse gas concentration levels, and the atmospheric carbon dioxide concentrations peak at >1,370 ppm (in 2100). In our experiment, the surface temperature products of the RCPs (RCP2.6/4.5/6.0/8.5, 2006–2100) developed by the Meteorological Research Institute, Japan (the Coupled Model Intercomparison Project, Phase5, CMIP5) were used (Yukimoto et al., 2012), which is available online (<https://esgf-node.llnl.gov/search/cmip5/>). The spatial resolution of the RCP products is about $1.12148^\circ \times 1.125^\circ$, and we used the monthly surface temperatures. The temperature of each basin was then obtained by averaging monthly surface temperature of all pixels located in the basin. In general, a lake often covers an area that is smaller than the spatial resolution of the monthly surface temperature. Moreover, lake ice phenology is affected by regional temperature (Yao et al., 2016). We therefore assigned the temperature of each basin to all the lakes in the corresponding basin.

2.3. Lake Attributes Data Set

Lake ice phenology is affected by both climate factors and attributes of the lake itself. In this study, the attributes (i.e., area, perimeter, elevation, latitude of lake center, and longitude of lake center) and lake shape were taken into consideration. We obtained the lake area, lake perimeter and calculated the lake shape from “The lakes larger than 1 km² in Tibetan Plateau (V2.0) (1970s–2018),” which is available at <https://data.tpdc.ac.cn/en/> (Zhang, 2019). The product provided a long and dense lake observations between the years of 1970s and 2018, including the data of 12 individual years (1970s, 1990, 1995, 2000, 2005, 2010, 2013, 2014, 2015, 2016, 2017, and 2018). The area and perimeter of 35 studied lakes are directly obtained from the data set. We further used two indicators (calculate compactness [CS] and calculate complexity [CP]) for the lake shape measurement which derived from the lake polygon (Brinkhoff et al., 1995). The CS and CP calculation code can be obtained online (<https://github.com/pondrejk/PolygonComplexity/>). The attributes of area, perimeter, CS, and CP of the studied lakes were obtained by averaging of the lake attribute data in 2005, 2010, 2013, 2014, and 2015. The central latitude and central longitude of lakes were got from lake ice phenology data set (Qiu et al., 2017). In terms of the lake elevation, the Shuttle Radar Topography Mission (SRTM) version 3 Digital Elevation Model (DEM) products were used (<https://dwtkns.com/srtm30m/>). The DEM

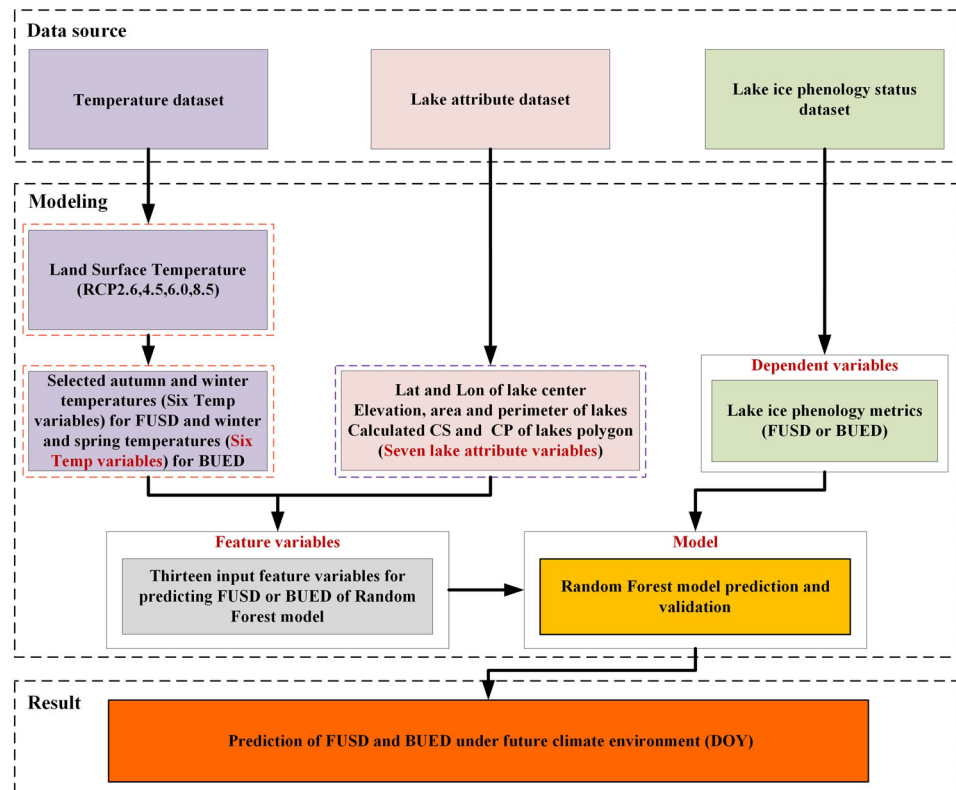


Figure 2. Flowchart of the proposed method for predicting lake ice freeze-up start date (FUSD) and break-up end date (BUED). DOY denotes the day of the year.

product is masked by the lake area data set, and then the elevation of each lake was calculated by averaging all pixels in each lake.

3. Methodology

3.1. Predicting FUSD and BUED Based on the RF Model

We employed the random forest (RF) regression model to predict the lake ice FUSD and BUED of each year. The RF regression model is one of the most effective machine learning models for predictive analysis, which randomly generates multiple non-associated decision trees and combines their results to control overfitting and to improve accuracy. As reported, random forest is robust to noise data (Breiman, 2001) and can deal with complex high-dimensional variables even if they are highly correlated (Criminisi et al., 2012). We employed the default parameters of the RF regression model in Scikit-learn (Pedregosa et al., 2011) for our experiments. The number of trees is 100. The maximum depth of the tree is determined as the nodes are expanded until all leaves are pure or until all leaves contain less than two samples. The framework to predict lake ice FUSD and BUED using random forest is shown in Figure 2.

The input data used for the RF regression model included the land surface temperature (LST) and lake attributes. Correspondingly, the lake ice phenology metrics derived from the lake ice phenology data set (Section 2.1) served as the model output (ground truth). We believe that the lake ice phenology is affected by short- and medium-term temperature changes, i.e., the temperatures in September, October, November, December, January, and February affect freeze-up start, while those in December, January, February, March, April, and May influence break-up end (Kropacek et al., 2013; Latifovic & Pouliot, 2007; Weber et al., 2016; Yao et al., 2016). Therefore, the temperatures of the related 6 months were used for FUSD and BUED prediction. For the lake attribute data, the central latitude, the central longitude, the elevation, the area, the perimeter, CS, and CP of each lake were used.

AMSR-E and AMSR2 did not provide continuous observations, and there was a data gap from October 2011 to July 2012. Moreover, the BUSD records of many lakes in 2016 were missing in the lake ice phenology data set. Therefore, we only used the available records of BUED and FUSD across 2002–2015 in the lake ice phenology data set for modeling. In addition, for a seasonal cycle of lake ice in the TP, BUED appears in the next year after FUSD. As such, the training samples of FUSD were from the years of 2006–2012 (except 2011 owing to the data gap), while samples from 2013 and 2014 were employed for model test. Correspondingly, the training samples of BUED were obtained from the years of 2007–2013 (except 2012 owing to the data gap), and samples from 2014 and 2015 were used for model test. The regression model is assessed by the following metrics: the coefficient of determination (R^2) (Nagelkerke, 1991), the root mean square error (RMSE), the mean absolute error (MAE) (Willmott, 1982), and the mean absolute percentage error (MAPE) (Goodwin & Lawton, 1999).

3.2. Trend Analysis

The trend of lake ice dynamics was analyzed by combining the methods of MK and Sen's slope estimator (Hewitt et al., 2018; Latifovic & Pouliot, 2007). The MK test is a non-parametric time series trend test method (Gocic & Trajkovic, 2013), which does not require the time series data to be normally distributed. Sen's slope estimator is a method for calculating the magnitude of a trend. It is calculated by the median of the time series, which can reduce the impact of outliers (Gocic & Trajkovic, 2013).

The statistic S in the MK test (Kendall, 1975; Mann, 1945) can be defined as

$$S = \sum_{i=1}^{n-1} \sum_{j=i+1}^n \text{sgn}(X_j - X_i), \quad (1)$$

where

$$\text{sgn}(X_j - X_i) = \begin{cases} 1, & \text{if } X_j - X_i > 0 \\ 0, & \text{if } X_j - X_i = 0 \\ -1, & \text{if } X_j - X_i < 0 \end{cases}, \quad (2)$$

where X_i and X_j are i th and j th time series values, $\text{sgn}(X_j - X_i)$ is determined by the value of $X_j - X_i$, and n is the number of data in the time series. Based on S , the trend test is then given by

$$Z_S = \begin{cases} \frac{S-1}{\sqrt{\text{Var}(S)}}, & \text{if } S > 0 \\ 0, & \text{if } S = 0 \\ \frac{S+1}{\sqrt{\text{Var}(S)}}, & \text{if } S < 0 \end{cases}, \quad (3)$$

where

$$\text{Var}(S) = \frac{n(n-1)(2n+5) - \sum_{i=1}^m t_i(t_i-1)(2t_i+5)}{18}, \quad (4)$$

where n is the number of data in the time series, m is the number of tied values, and t_i denotes the number of ties of the i th value.

Given a specific α significance level, a significant trend exists when $|Z_S| > Z_{1-\alpha/2}$. In this study, we selected the significance level $\alpha = 0.05$, i.e., $Z_{1-\alpha/2} = Z_{0.975} = 1.96$.

$$\text{Trend} = \begin{cases} 1, & \text{if } |Z_S| > Z_{1-\alpha/2} \text{ and } Z_S > 0 \\ 0, & \text{if } |Z_S| < Z_{1-\alpha/2} \\ -1, & \text{if } |Z_S| > Z_{1-\alpha/2} \text{ and } Z_S < 0 \end{cases}. \quad (5)$$

Sen's slope was calculated to capture the magnitude of the trend (Sen, 1968):

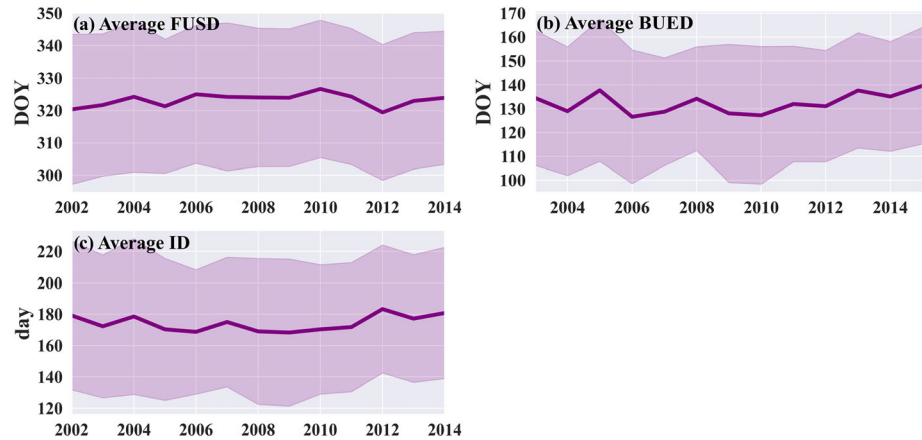


Figure 3. The average FUSD, BUED, and ID of the 35 studied lakes observed from 2002 to 2015. (a) Average FUSD from 2002 to 2014, (b) Average BUED from 2003 to 2015, and (c) Average ID from 2002 to 2014. Note that the FUSD in 2011 and the BUED in 2012 were obtained through random forest model simulation. The DOY denotes day of the year, and the shaded areas denotes the standard deviation of the average FUSD, BUED, and ID.

$$\beta = \text{Median}\left(\frac{X_j - X_k}{j - k}\right) \forall k < j, \quad (6)$$

where X_j and X_k are j th and k th time series values and $j > k$.

4. Results

4.1. Lake Ice Phenology and Dynamics Observed by Satellite Data

Figure 3 exhibits the average FUSD, BUED, and ID of the 35 studied lakes derived from satellite data. The lake ice dynamics trends over 2002–2015 across the 35 lakes were analyzed using statistical tests based on AMSR-E and AMSR2 satellite data (Table 1). The bold numbers in Table 1 indicate significant trends under the MK test. Five lakes (Bairab Co, Bamco, Kusai Lake, Margai Caka, and Memar Co) indicate increasing trends, which means that the FUSD of these lakes was delayed over 2002–2014. In terms of BUED, four lakes (Ayakkum Lake, Dogaicoring Qangco, Dorsoidong Co, and Lexiewudan Co) show significant increasing trends and one lake (Yuye Lake) shows a significant decreasing trend across 2003–2015. Additionally, ice duration (ID) is observed, among which three lakes (Ayakkum Lake, Lexiewudan Co, and Zhari Namco) show significant increasing trends (i.e., the lake ice duration is enlarged) while three lakes (Bairab Co, Norma Co, and Yuye Lake) show decreasing trends (i.e., the lake ice duration is shortened). In general, most of the lakes in the TP region did not show the trend of early break up and shortened ice cover duration from 2002 to 2015. Moreover, we found that the average FUSD ($\beta = 0.05$ days/yr, Trend = 0), the average BUED ($\beta = 0.47$ days/yr, Trend = 0), and the average ID ($\beta = 0.23$ days/yr, Trend = 0) show insignificant change trends. Overall, most of the lakes in the inner TP did not show significant lake ice phenology trends across the past few years based on the MK test.

4.2. Simulation of Lake Ice Phenology Based on the RF Regression Model

We used 13 variables, i.e., the temperatures derived from RCPs (temperatures of the 6 months in autumn and winter for FUSD, and those in winter and spring for BUED, respectively), the central latitude and the central longitude of each lake, lake area, lake perimeter, lake elevation, and lake shape indicators (CS and CP) as the input of the RF simulation. Figure 4 shows the performances of the RF simulation based on different LSTs in RCPs. Figures 4a–4d display the lake ice FUSD predicted under four RCP scenarios, while Figures 4e–4h show the predicted lake ice BUED. It can be seen that good simulation results of FUSD were obtained ($R^2 > 0.91$). In terms of BUED, slightly lower correlations with reference data were obtained for all scenarios ($R^2 > 0.84$) except under RCP4.5 ($R^2 = 0.74$). We used three metrics (i.e., RMSE, MAE, and MAPE) to evaluate the performance of the RF on predicting FUSD and BUED (as listed in Table 2). Good results are obtained for FUSD, as the RMSE is about 6 days, the MAE is about 5 days, and MAPE is less than 2%

Table 1
Lake Ice Dynamics Trends Across the 35 Lakes Estimated by the Mann-Kendall (MK) Test and Sen's Slope Based on AMSR-E and AMSR2 Satellite Data Over 2002–2015

Lake name	FUSD		BUED		ID	
	β	T	β	T	β	T
Aksayqin Hu	0.20	0	0.00	0	-0.26	0
Aqqikkol Lake	-0.27	0	0.53	0	0.67	0
Ayakkum Lake	-1.13	0	4.00	1	5.37	1
Bairab Co	1.43	1	0.26	0	-0.82	-1
Bamco	0.55	1	0.61	0	-0.17	0
Chibzhang Co	-1.13	0	-0.68	0	0.21	0
Dagze Co	0.10	0	0.23	0	0.43	0
Dogaicoring Qangco	-0.13	0	0.94	1	0.81	0
Dorsoidong Co	-0.10	0	2.00	1	2.10	0
Dulishi Lake	0.63	0	0.00	0	-0.62	0
Dung Co	0.00	0	0.92	0	1.38	0
Heishi North Lake	0.00	0	0.36	0	-0.29	0
Hoh Xil Lake	0.50	0	0.00	0	-0.18	0
Kusai Lake	0.50	1	-0.23	0	-0.78	0
Kyebxang Co	0.00	0	0.00	0	0.00	0
Lexiewudan Co	-1.00	0	2.70	1	2.89	1
Lumajiangdong Co	0.53	0	0.00	0	-0.42	0
Luotuo Lake	0.50	0	1.62	0	0.69	0
Margai Caka	0.58	1	-0.54	0	-0.96	0
Memar Co	0.85	1	-0.10	0	-1.40	0
Nam Co	0.00	0	0.08	0	0.00	0
Ngangla Ringco	-0.67	0	1.00	0	1.46	0
Ngangze Co	-0.13	0	0.67	0	0.70	0
Norma Co	0.50	0	-1.18	0	-1.50	-1
Pung Co	0.75	0	0.92	0	-0.49	0
Rinqin Xubco	0.17	0	1.00	0	0.60	0
Rola Co	0.29	0	0.27	0	0.32	0
Selin Co	0.23	0	0.14	0	-0.23	0
Wulanwula Lake	0.21	0	0.86	0	0.58	0
Xiangyang Lake	0.50	0	1.20	0	0.41	0
Yanghu Lake	0.69	0	0.17	0	-0.58	0
Yuye Lake	-0.24	0	-2.17	-1	-2.18	-1
Zhari Namco	-0.44	0	0.62	0	1.00	1
Zhuonai Lake	-0.63	0	-0.33	0	0.15	0
Zige Tangco	0.50	0	0.73	0	0.00	0

Note: The FUSD in 2011 and the BUED in 2012 were obtained through random forest model simulation. The β denotes Sen's slope and T denotes the MK test result of the time serial data (the location and some characteristics of the lakes are shown in Table S1). The bold numbers in Table indicate significant trends under the MK test.

under all RCPs. Slightly errors was achieved for BUED, as the RMSE is about 12 days, the MAE is about 10 days, and MAPE is less than 9% under all RCPs. Overall, the RF regression provide a mean to simulate lake ice phenology.

Based on the trained RF regression model, we predicted the lake ice FUSD/BUED of the studied 35 lakes in the TP in the future climate scenarios via the input variables of the years 2015–2098/2016–2099. Figure 5a shows the average temperatures from September to next February over the period of 2015 to 2098, and Figure 5b shows those from December to next May over 2016 to 2099. Owing to the low greenhouse gas concentration, temperature under RCP2.6 fluctuates with no obvious upward trend. RCP4.5 and RCP6.0 show a slight upward trend, while RCP8.5 has a significant temperature rising trend. Although differences exist, the temperature changes in a zigzag pattern across the whole century under different scenarios, which implies a small cycle of climate with the alternating of cold and warm every few years. Lake ice phenology changes with temperature variation. Overall, the advance of BUED and the delay of FUSD result in shortened ice duration. Similar to temperature, lake ice phenology shows a large cycle period overlapped by several small cycle periods. In particular, the average FUSD shows a relatively gentle change after the year 2060 compared with the latter years under RCP8.5. The change of temperature caused the change in FUSD. We also report the average FUSD, BUED, and ID of the six sub-basins over the time period of 2002–2099 (Table 3).

4.3. The Lake Ice Phenology Dynamics in the Future Climate Scenarios

The predicted lake ice phenology dynamics was analyzed. Figure 6 shows the spatial distribution of Sen's slope for both FUSD and BUED in 2002–2099 under four RCP scenarios. The red triangle indicates an increasing trend, the blue triangle denotes a decreasing trend, and the purple cross means that the trend is significant. Figures 6a–6d show Sen's slopes of FUSD under RCP2.6/4.5/6.0/8.5. Inners D, E, and F indicate increasing trends, which means that the FUSDs of the lakes are delayed. Among the lakes with significant changes in FUSD, more than 75.68% of them show freeze-up starting delays under different RCPs (Table 4). Meanwhile, FUSDs in Inners A, B, and C are relatively stable with Sen's slope varying from -0.01 to 0.01. Figures 6e–6h show Sen's slopes of BUED. Most lakes under the RCP scenarios, except RCP2.6, have decreasing trends, which means that the BUEDs of the lakes are advanced. Among the lakes with significant changes in BUED, 96.30%

of the lakes show break-up ending advances. Similarly, the ice durations of most of the studied lakes are shortened, except under RCP2.6 (Figures 6i–6l). In general, the simulation results of long-term lake ice phenology (2002–2099) of 35 lakes show that the average FUSD is significantly delayed, while the average BUED is significantly advanced, except for RCP2.6. Accordingly, the average ice duration is shortened, especially for the lakes in the northern part of the study area.

Table 5 reports lake ice phenology changes in the six sub-basins under different RCPs. Among the six studied sub-basins, the average FUSD change in Inner B is not significant under all climate scenarios. Inners A, C, and D only show significant changes under one climate scenario (Inner A delayed under RCP4.5, Inner C advanced, and Inner D delayed under RCP6.0). The average FUSD changes in Inners E and F are significantly delayed under all climate scenarios except RCP2.6. Compared with the other regions, the FUSD dynamics of Inner E is the largest, which is delayed by 0.03 days/yr, 0.05 days/yr, and 0.11 days/yr from 2002 to 2098 under RCP4.5, RCP6.0, and RCP8.5, respectively. In terms of average BUED, Inners B, C, D,

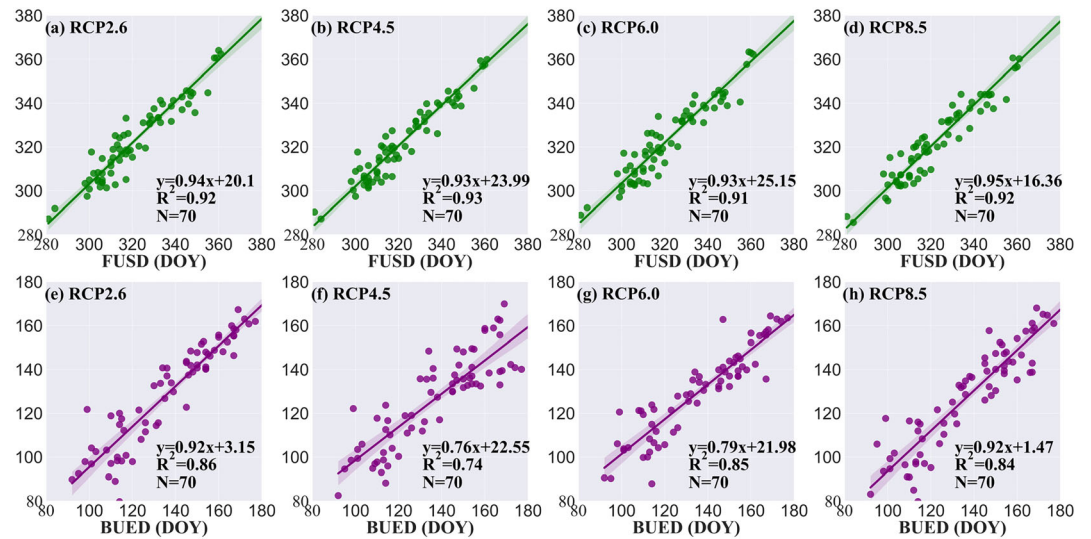


Figure 4. Lake ice FUSD and BUED predictions based on the random forest (RF) regression model. (a–d) the predicted FUSD prediction with input temperatures variables of RCP2.5/4.5/6.0/8.5 LST (autumn and winter), respectively, against reference; (e–h) the BUED prediction results with input temp variables of RCP2.5/4.5/6.0/8.5 LST (winter and spring), respectively, against reference. DOY denotes day of the year. The shaded areas denote the confidence interval (ci = 95%) for the regression estimation.

E, and F are significantly advanced under RCP6.0 and RCP8.5. Inner E has the largest BUED changes, with the size of -0.04 , -0.11 , and -0.32 days/yr from 2003 to 2099 under RCP4.5, RCP6.0, and RCP8.5, respectively. Results in Inner F were similar to those in Inner E. Due to the changes in FUSD and BUED, most average IDs of the six sub-basins are shortened significantly under the RCP4.5, RCP6.0, and RCP8.5. Inevitably, the maximum average ID change is in Inner E, which is shortened by -0.07 , -0.18 , and -0.43 days/yr from 2002 to 2098 under RCP4.5, RCP6.0, and RCP8.5. In addition, we calculated the average changes for FUSD, BUED, and ID of 35 selected lakes during the period of 2012–2099. As listed in Table 6, the average FUSD of the 35 studied lakes is delayed by 0.01, 0.04, and 0.04 days/yr from 2002 to 2098 under RCP4.5, RCP6.0, and RCP8.5, respectively, while the average BUED is advanced by 0.04, 0.11, and 0.21 days/yr from 2003 to 2099, respectively. The average ice duration of 35 lakes shortened by 0.05, 0.14, and 0.25 days/yr from 2002 to 2098 under RCP4.5, RCP6.0, and RCP8.5, respectively.

Sen's slopes of the middle-term (2002–2050) and long-term (2002–2099) periods are shown in Figure 7. They show a similar trend under RCP2.6/4.5/6.0/8.5. Sen's slope of the middle-term is larger than that of the long-term, indicating that the FUSD of lakes in the TP show obvious change in the period of 2002–2050 and gradually become stable in the later period (2051–2099).

5. Discussion

5.1. Feature Importance Analysis of FUSD and BUED Prediction

In this study, we employed an RF regression model to predict FUSD and BUED based on LST and lake attribute data, obtaining acceptable results. We investigated the variable importance in prediction, to understand how the lake attributes and LST impact lake ice phenology. For simplicity, we analyze the parameter importance for the RCP8.5 climate scenario. Figure 8 shows the Gini Importance ranking among the 13 variables. The Gini Importance was used to calculate the importance of a feature, which is computed as the (normalized) total reduction of the criterion brought by that feature (Pedregosa et al., 2011). Figure 8a shows the top five important variables for lake ice FUSD prediction, i.e., lake latitude, lake area, surface temperature in September, lake perimeter, and

Table 2
The Statistical Metrics Related to the Lake Ice FUSD and BUED Predictions Using the Random Forest (RF) Model

Metrics	Climate scenarios	R^2	RMSE (days)	MAE (days)	MAPE (%)
FUSD	RCP2.6	0.92	6.20	4.81	1.50
	RCP4.5	0.93	5.52	4.37	1.37
	RCP6.0	0.91	6.45	5.00	1.56
	RCP8.5	0.92	5.93	4.77	1.48
BUED	RCP2.6	0.86	11.50	9.19	6.89
	RCP4.5	0.74	15.85	12.70	9.08
	RCP6.0	0.85	11.27	9.57	6.98
	RCP8.5	0.84	13.51	10.81	8.09

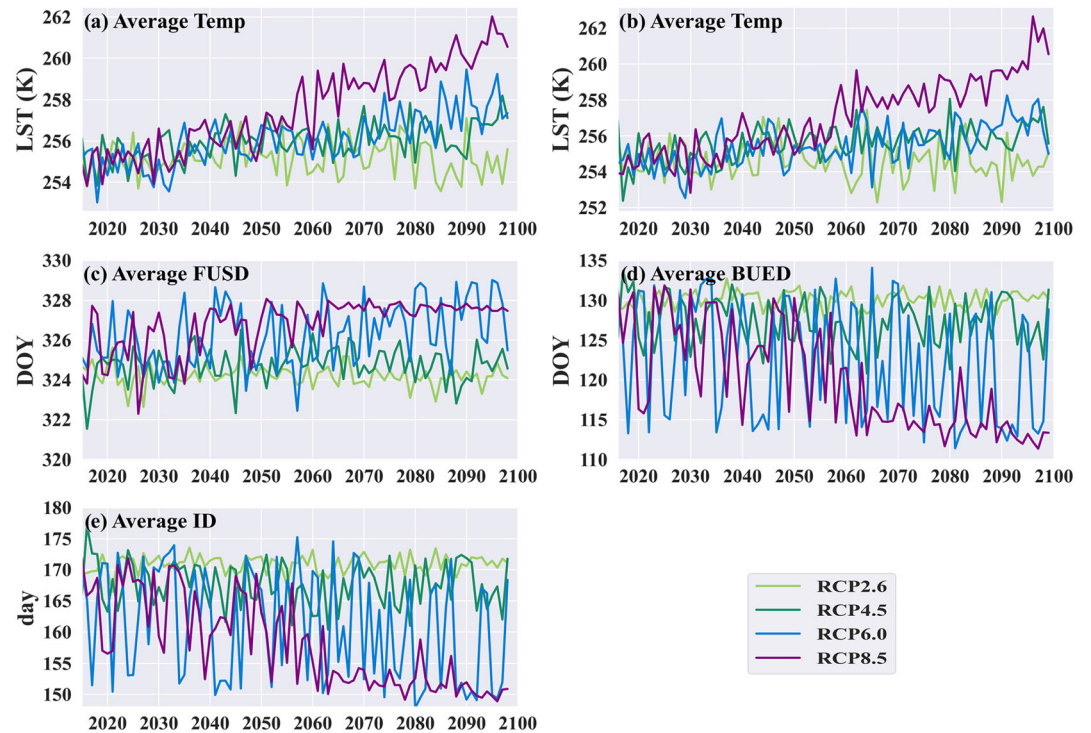


Figure 5. The average temperature in the inner TP and the average FUSD, BUED, and ID of the 35 studied lakes from 2015 to 2099. The figures shows (a) average temperature in September, and October and November, December, January, and February from 2015 to 2098. (b) Average temperature in December, January, February, March, April, and May from 2016 to 2099. (c) Average FUSD from 2015 to 2098; (d) average BUED from 2016 to 2099; and (e) average ID from 2015 to 2098. The DOY denotes day of the year, and LST denotes the land surface temperature.

surface temperature in October. Figure 8b shows that the top five important variables for lake ice BUED prediction are the surface temperature in March, lake elevation, lake latitude, surface temperature in April, and lake area. Figure 8 illustrates that lake latitude and surface temperature are the most important variables in the RF model for predicting lake ice FUSD and BUED, respectively.

5.2. Effect of Lake Attributes on Inter-Annual Variation of Lake Ice Phenology (Sen's Slope)

In general, the simulation results showed that lakes are inclined to freeze-up later and break up earlier in the future decades, as reported in section 4 (Figure 5). However, the pace of lake ice phenology changes showed

Table 3

Statistics on the Average FUSD, and ID During the Period of 2002–2098 and the Average BUED During the Period of 2003–2099 as Derived From Satellite Observation and the Random Forest Model Simulation Under Different RCPs in the Six Sub-Basins

Metrics	Scenarios	Inner A	Inner B	Inner C	Inner D	Inner E	Inner F
FUSD	RCP2.6	341.41 ± 1.70	361.66 ± 1.96	343.87 ± 2.17	329.81 ± 2.69	307.58 ± 1.65	313.79 ± 1.52
	RCP4.5	342.34 ± 1.42	361.50 ± 2.11	344.60 ± 2.62	331.30 ± 3.25	308.64 ± 2.63	316.18 ± 2.71
	RCP6.0	341.19 ± 1.00	361.72 ± 1.80	343.52 ± 2.06	331.21 ± 2.62	310.20 ± 2.56	316.84 ± 2.04
	RCP8.5	340.89 ± 0.85	362.09 ± 1.74	344.73 ± 1.99	331.35 ± 2.65	312.62 ± 3.94	317.84 ± 2.68
BUED	RCP2.6	104.61 ± 2.84	99.61 ± 3.51	116.80 ± 3.85	109.97 ± 4.76	148.02 ± 2.61	147.66 ± 3.06
	RCP4.5	105.81 ± 2.83	101.17 ± 3.91	116.47 ± 4.30	105.26 ± 6.78	145.91 ± 6.36	144.02 ± 6.68
	RCP6.0	103.91 ± 4.21	98.22 ± 6.93	115.57 ± 6.24	106.15 ± 9.32	140.31 ± 10.07	137.73 ± 10.64
	RCP8.5	101.85 ± 2.84	96.51 ± 4.34	112.85 ± 4.90	105.97 ± 6.10	137.60 ± 10.77	134.06 ± 10.98
ID	RCP2.6	128.20 ± 2.90	102.94 ± 3.78	137.92 ± 4.68	145.16 ± 6.65	205.44 ± 3.61	198.88 ± 3.75
	RCP4.5	128.47 ± 2.87	104.67 ± 4.19	136.86 ± 5.56	138.95 ± 9.40	202.27 ± 8.56	192.84 ± 8.95
	RCP6.0	127.72 ± 4.08	101.51 ± 7.12	137.05 ± 6.75	139.94 ± 10.93	195.11 ± 11.98	185.88 ± 12.11
	RCP8.5	125.96 ± 2.60	99.42 ± 4.55	133.12 ± 5.46	139.62 ± 7.73	189.97 ± 13.99	181.23 ± 12.94

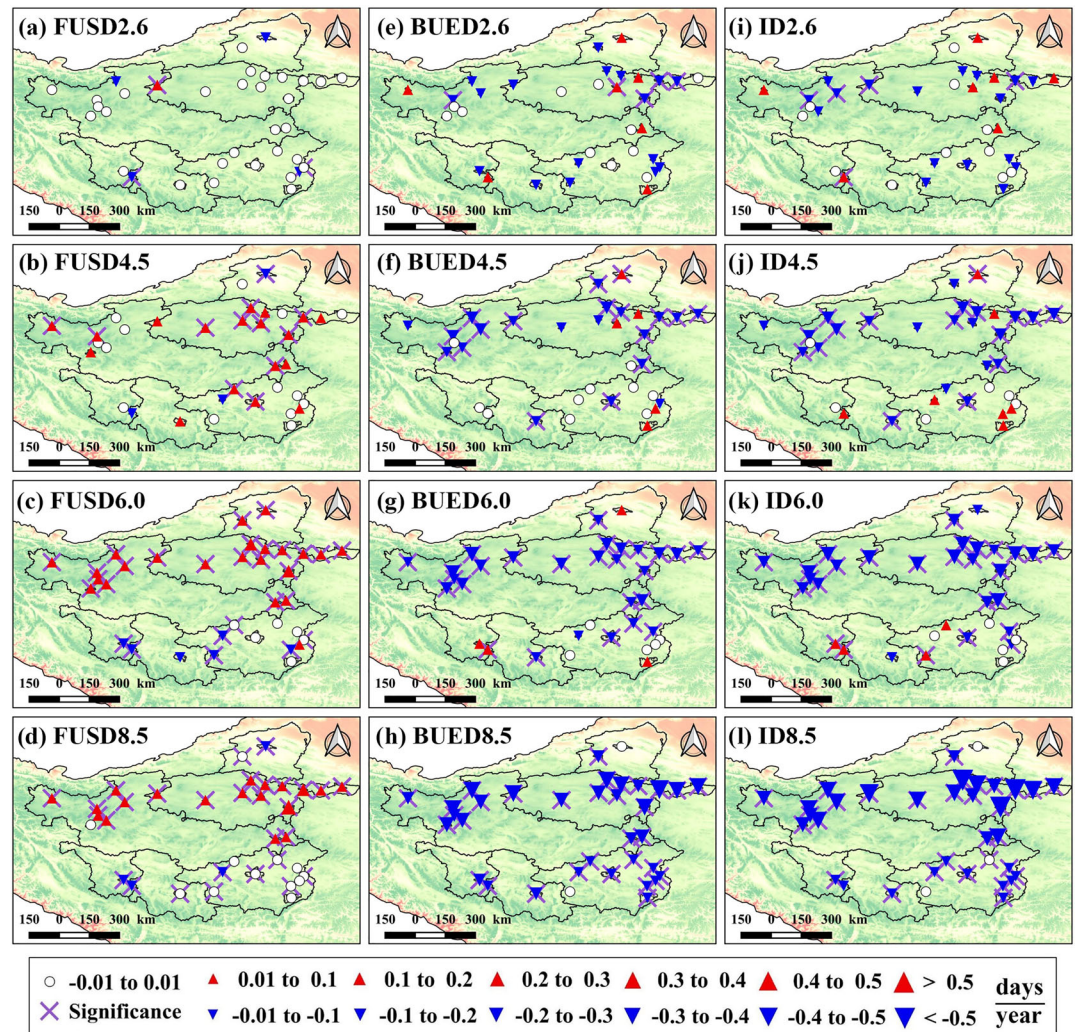


Figure 6. The spatial distribution maps of the Mann-Kendall test and Sen's slope estimator from the prediction of lake ice phenology under different RCP climate scenarios from 2002 to 2098 or 2003 to 2099. (a–d) the predicted FUSD with input from RCP2.6, RCP4.5, RCP6.0, and RCP8.5 (2002 to 2098), respectively; (e–h) the predicted BUED with input from RCP2.6, RCP4.5, RCP6.0, and RCP8.5 (2003 to 2099), respectively; (i–l) the predicted ID with input from RCP2.6, RCP4.5, RCP6.0, and RCP8.5 (2002 to 2098), respectively. Note that the input variable of lake area is constant.

significantly different characteristics across the six sub-basins on the TP. Taking FUSD8.5 as an example, the FUSD of lakes changes more violently in regions with higher altitude and elevation than those at lower altitude and elevation (Figure 6). To better show the results and latent rules, we also visualized the distribution of FUSD8.5 changes with different lake attributes using Sen's slope (Figure 9). The difference between the average lake elevation when Sen's slope ≥ 0 and average lake elevation when Sen's slope < 0

Table 4
The Numbers of Lakes With Significant Trends by Sen's Slope Estimator for the Predicted FUSD, BUED, and ID During the Period of 2002–2099

Number	FUSD delayed lakes with significance	FUSD changed lakes with significance	BUED advanced lakes with significance	BUED changed lakes with significance	ID shortened lakes with significance	ID changed lakes with significance
RCP2.6	2	3	4	5	4	5
RCP4.5	11	12	16	17	16	17
RCP6.0	22	29	25	26	24	27
RCP8.5	21	30	33	33	32	32

Table 5
Sen's Slope and Mann-Kendall (MK) Tests of Average Lake Ice Phenology Changes in the Six Sub-Basins From 2002 to 2099 Under Different RCPs

Metrics	Scenarios	Inner A		Inner B		Inner C		Inner D		Inner E		Inner F	
		β	T	β	T	β	T	β	T	β	T	β	T
FUSD	RCP2.6	0	0	0.01	0	0	0	0	0	0.01	0	0	0
	RCP4.5	0.02	1	0.01	0	0.01	0	0	0	0.03	1	0.03	1
	RCP6.0	0	0	0	0	-0.01	-1	0.02	1	0.05	1	0.04	1
	RCP8.5	0	0	0	0	0	0	0	0	0.11	1	0.06	1
BUED	RCP2.6	-0.01	0	0	0	0.02	0	0.01	1	0	0	-0.01	0
	RCP4.5	-0.01	0	-0.02	0	-0.03	0	-0.01	0	-0.04	-1	-0.04	0
	RCP6.0	-0.02	0	-0.07	-1	-0.06	-1	-0.05	-1	-0.11	-1	-0.11	-1
	RCP8.5	0	0	-0.06	-1	-0.08	-1	-0.1	-1	-0.32	-1	-0.31	-1
ID	RCP2.6	-0.01	0	0	0	0.03	0	0.03	0	-0.01	0	-0.01	0
	RCP4.5	-0.03	-1	-0.03	0	-0.03	-1	-0.01	0	-0.07	-1	-0.08	-1
	RCP6.0	-0.02	-1	-0.08	-1	-0.05	-1	-0.08	-1	-0.18	-1	-0.17	-1
	RCP8.5	0	0	-0.05	-1	-0.08	-1	-0.11	-1	-0.43	-1	-0.38	-1

Note: β denotes Sen's slope and T denotes the MK test result of the time serial data.

is approximately 204.01 m, while that of the central latitude is 1.66°. In particular, lakes with Sen's slope >0.1 have shown relatively large differences in elevation and latitude from other lakes. Almost all of them are located in high elevation and high latitude areas. Lakes with high elevation and latitude show an upward trend (Sen's slope >0, FUSD delayed) in terms of freezing up. We reviewed the lakes and found that most of them were located in Inners E and F. However, most of the lakes' FUSD in Inners A, B, and C (low elevation and latitude) remained unapparent (Sen's slope = 0, unchanged), and only a few lakes showed a downward trend (Sen's slope <0, FUSD advanced). The reason may be that high elevation/latitude lakes are highly vulnerable to climate warming (Preston et al., 2016); the rate of temperature increase is amplified in these regions. The lakes located in Inners E and F are expected to be more sensitive to temperature rises than those in Inners A, B, and C with low elevation/latitude. In terms of lake area, we found that four lakes with very large areas (Nam Co 2,019.20 km², Nam Co 2,019.70 km², Ayakkum Lake 936.69 km², and Zhari Namco 1,005.50 km²) fall into the group of Sen's slope <0.01. Large lakes with areas close to or greater than 1,000 km² are more likely to resist the effects of climate change, showing better anti-climate interference characteristics than small ones.

5.3. Uncertainties

Uncertainties existed in the lake ice phenology prediction, which may have affected the results. The uncertainties mainly come from two aspects, i.e., the RF model and the input data. In this paper, we focused on the discussion of the input data, and the uncertainties caused by the systematic error of the model are not considered. The lake ice phenology data set and lake attributes data set often have ineluctable uncertainties when they are retrieved from satellite remote sensing data. Other lake attributes, such as lake depth and salinity, are closely related to lake ice phenology. However, we cannot involve them in RF modeling because of the lack of data. In this research, we applied the monthly surface temperature with a spatial resolution of approximately 1.12148° × 1.125° from RCPs products for lake ice phenology simulation. A higher spatial and temporal resolution of the surface temperature data is more conducive to the simulation.

Based on the RF model, we estimated that the lake ice freeze-up of 35 studied lakes were delayed by an average of 0.01, 0.04, and 0.04 days/yr from 2002 to 2098 under RCP4.5, RCP6.0, and RCP8.5, respectively, whereas the break-up advanced by an average of 0.04, 0.11, and 0.21 days/yr from 2003 to 2099. Accordingly, the average ID of the 35 studied lakes decreased by 0.05, 0.14, and 0.25 days/yr from 2002 to 2098 under

Table 6
Sen's Slope and Mann-Kendall (MK) Tests of Average Lake Ice Phenology Changes of the 35 Studied Lakes From 2002 to 2099 Under the Different RCPs

Metrics	MK-Sen's slope	RCP2.6	RCP4.5	RCP6.0	RCP8.5
		FUSD (days/yr)	Slope	0.0009	0.01
	T	0	1	1	1
BUED (days/yr)	Slope	-0.002	-0.04	-0.11	-0.21
	T	0	-1	-1	-1
ID (days/yr)	Slope	-0.003	-0.05	-0.14	-0.25
	T	0	-1	-1	-1

Note: β denotes Sen's slope and T denotes the MK test result of the time serial data.

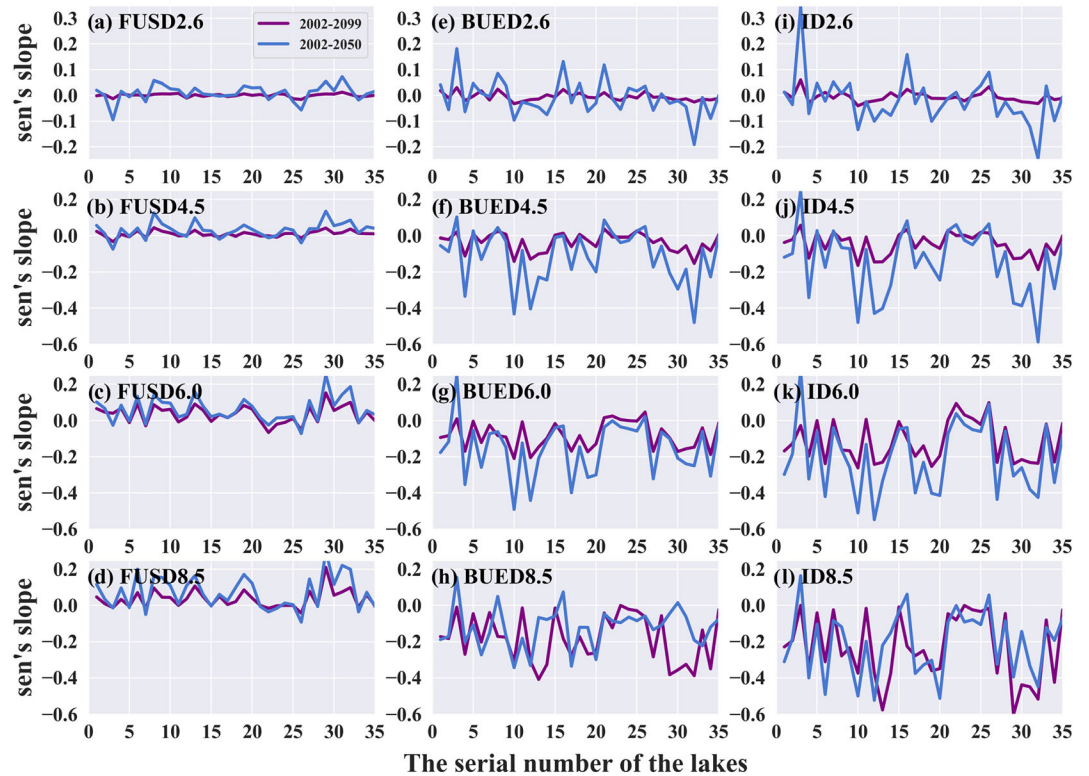


Figure 7. Comparisons among the predicted lake ice FUSD, BUED, and ID under different future climate scenarios; (a–d) Sen's slope of FUSD under RCP2.6/RCP4.5/RCP6.0/RCP8.5, respectively; (e–h) Sen's slope of BUED under RCP2.6/RCP4.5/RCP6.0/RCP8.5, respectively; (i–l) Sen's slope of ID under RCP2.6/RCP4.5/RCP6.0/RCP8.5, respectively. The serial number of the lakes is sorted by the initials of the lake's name (as listed in Table 1).

RCP4.5, RCP6.0, and RCP8.5, respectively. Although the annual change rate of lake ice phenology is small, the cumulative effect of time cannot be ignored. In detail, the average ID of the 35 studied lakes decreased by 4.85, 13.58, and 24.25 days from 2002 to 2098 under RCP4.5, RCP6.0, and RCP8.5. On the other hand, the change rate is averaged over the six sub-basins. However, the ID in some sub-basins is not shortened, as reported in Table 5. This means that the ID change rate in some sub-basins is often larger than the average change rate we reported. For example, the average ID in Inner E was shortened by 6.79, 17.46, and 41.71 days from 2002 to 2098 under RCP4.5, RCP6.0, and RCP8.5, respectively.

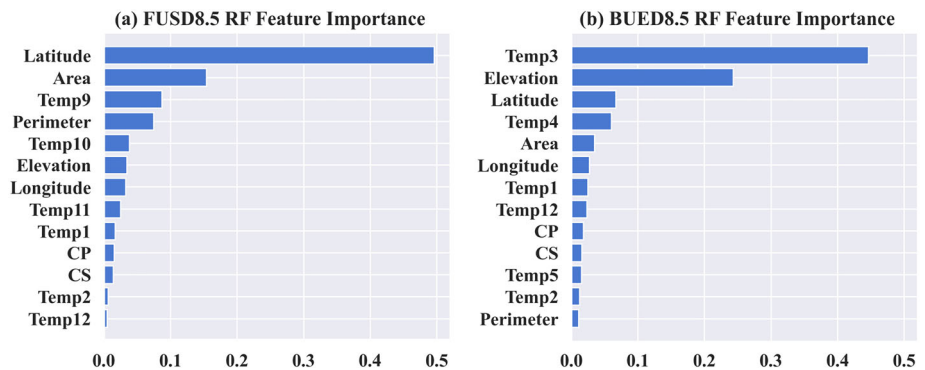


Figure 8. Gini importance of the 13 variables in lake ice FUSD and BUED predictions under RCP8.5 climate scenario; (a) feature importance in FUSD prediction with RF model and (b) feature importance in BUED prediction with RF model. Temp1 denotes the surface temperature in January, Temp2 for February, Temp3 for March, etc.

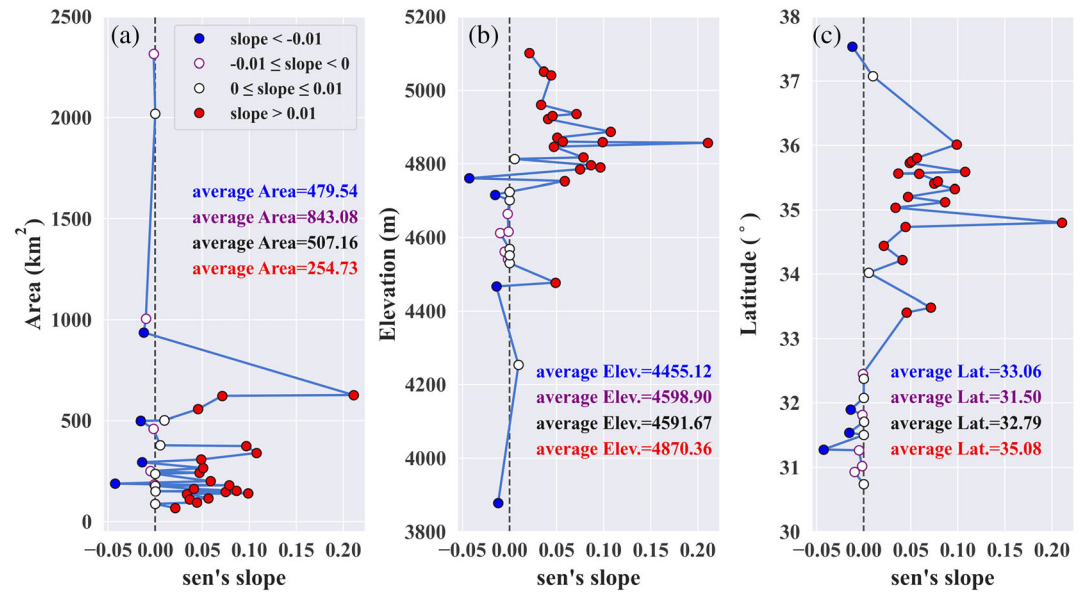


Figure 9. Distribution of FUSD Sen's slope change with different lake attributes under the RCP8.5 climate scenario. Blue points represent the result of Sen's slope less than -0.01 ; purple hollow points represent the result of Sen's slope greater than or equal to -0.01 and less than 0 ; white points with black circle represent the result of Sen's slope greater than or equal to 0 and less than or equal to 0.01 ; and red points represent the result of Sen's slope greater than 0.01 . The lakes were divided into two groups and then the serial number of the lakes were sorted by name (as listed in Table 1).

6. Conclusion

In this paper, we presented an RF regression method for lake ice phenology simulation under different RCPs, and we analyzed lake ice phenology trends. The experimental results show that FUSD and BUED are well simulated by the RF model with high correlations between predicted and reference data ($R^2_{\text{FUSD}} > 0.91$ under the different RCPs, and $R^2_{\text{BUED}} > 0.84$, except in the case of RCP2.6).

Under the background of climate change, the average FUSD of the 35 studied lakes could delay by 0.01, 0.04, and 0.04 days/yr from 2002 to 2098 under RCP4.5, RCP6.0, and RCP8.5, respectively, while the average BUED could advance by 0.04, 0.11, and 0.21 days/yr from 2003 to 2099 under RCP4.5, RCP6.0, and RCP8.5, respectively. Lake ice phenology changes in response to the rising of LST, the advance of BUED, and the delay of FUSD resulted in the shortening of ice duration. The average ice duration of the 35 studied lakes shortened by 0.05, 0.14, and 0.25 days/yr from 2002 to 2098 under RCP4.5, RCP6.0, and RCP8.5, respectively.

The temperature change impacts lake phenology under different RCP scenarios, and the impacts was larger in the early period (2002–2050) than in the later period (2050–2099). Lake ice phenology change was also affected by lake attributes. These results indicate that the lake ice phenology changes may be more fierce in the high latitude and high altitude area of the inner TP.

The results of this study can provide a better understanding of climate change research in the inner TP region and of the future lake ice phenology changes in the TP. This research can also provide decision support to deal with climate change, such as in managing the reduction of ice duration and the release of greenhouse gases (CO_2 , CH_4 , etc.) from the bottom of the lake.

Data Availability Statement

The lake ice phenology data set is available online (<http://www.csdata.org/en/p/105/>). The surface temperature products of the RCPs are available online (<https://esgf-node.llnl.gov/search/cmip5/>). The RCPs products can be obtained by searching. We used four search keywords (Model = "MRI-CGCM3," Experiment Family = "RCP," Time Frequency = "mon," and Variable = "ts") to filter out the surface temperature products under four RCPs (more details as shown in Figure S1). The lake attributes data set is provided by

National Tibetan Plateau Data Center (<https://doi.org/10.11888/Hydro.tpcd.270303>). The SRTM version 3 DEM products are available online (<https://dwtkns.com/srtm30m/>).

Acknowledgments

This research is supported by National Key R&D Program of China (grant no. 2018YFB2100702), Strategic Priority Research Program of the Chinese Academy of Sciences (grant no. XDA19070201), National Key R&D Program of China (grant no. 2017YFA0604300), National Natural Science Foundation of China (grant nos. 41875122 and 42071441), Western Talent (grant no. 2018XBYJRC004), and Guangdong Top Young Talents of Science and Technology (grant no. 2017TQ04Z359). We thank the lake ice phenology data set, Lake attributes data set, and SRTM Version 3 DEM production researcher. We thank anonymous reviewers for their constructive comments.

References

Benson, B., Magnuson, J., & Sharma, S. (2000). *Global lake and river ice phenology database, Version 1*. Boulder, Colorado USA: NSIDC: National Snow and Ice Data Center. <https://doi.org/10.7265/N5W66HP8>

Breiman, L. (2001). Random forests. *Machine Learning*, 45(1), 5–32. <https://doi.org/10.1023/A:1010933404324>

Brinkhoff, T., Kriegel, H.-P., Schneider, R., & Braun, A. (1995). *Measuring the complexity of polygonal objects* (pp. 109). Baltimore, MD: ACM-GIS.

Cai, Y., Ke, C. Q., & Duan, Z. (2017). Monitoring ice variations in Qinghai Lake from 1979 to 2016 using passive microwave remote sensing data. *Science of the Total Environment*, 607–608, 120–131. <https://doi.org/10.1016/j.scitotenv.2017.07.027>

Cai, Y., Ke, C. Q., Li, X., Zhang, G., Duan, Z., & Lee, H. (2019). Variations of lake ice phenology on the Tibetan Plateau from 2001 to 2017 based on MODIS data. *Journal of Geophysical Research: Atmospheres*, 124, 825–843. <https://doi.org/10.1029/2018JD028993>

Che, T., Li, X., & Jin, R. (2009). Monitoring the frozen duration of Qinghai Lake using satellite passive microwave remote sensing low frequency data. *Chinese Science Bulletin*, 54(13), 2294–2299. <https://doi.org/10.1007/s11434-009-0044-3>

Criminisi, A., Shotton, J., & Konukoglu, E. (2012). Decision forests: A unified framework for classification, regression, density estimation, manifold learning and semi-supervised learning. *Foundations Trends® in Computer Graphics Vision*, 7(2–3), 81–227. <https://doi.org/10.1561/06000000035>

Crossman, J., Eimers, M. C., Kerr, J. G., & Yao, H. (2016). Sensitivity of physical lake processes to climate change within a large Precambrian Shield catchment. *Hydrological Processes*, 30(23), 4353–4366. <https://doi.org/10.1002/hyp.10915>

Du, J., & Kimball, J. S. (2018). *Daily lake ice phenology time series derived from AMSR-E and AMSR2, Version 1*. Boulder, Colorado USA: NASA National Snow and Ice Data Center Distributed Active Archive Center. <https://doi.org/10.5067/HT4NQ07ZJF7M>

Gocic, M., & Trajkovic, S. (2013). Analysis of changes in meteorological variables using Mann-Kendall and Sen’s slope estimator statistical tests in Serbia. *Global and Planetary Change*, 100, 172–182. <https://doi.org/10.1016/j.gloplacha.2012.10.014>

Goodwin, P., & Lawton, R. (1999). On the asymmetry of the symmetric MAPE. *International Journal of Forecasting*, 15(4), 405–408. [https://doi.org/10.1016/S0169-2070\(99\)00007-2](https://doi.org/10.1016/S0169-2070(99)00007-2)

Gou, P., Ye, Q., Che, T., Feng, Q., Ding, B., Lin, C., & Zong, J. (2017). Lake ice phenology of Nam Co, central Tibetan Plateau, China, derived from multiple MODIS data products. *Journal of Great Lakes Research*, 43(6), 989–998. <https://doi.org/10.1016/j.jglr.2017.08.011>

Hartmann, D., Tank, A., & Rusticucci, M. J. I. A. (2013). *IPCC fifth assessment report, climate change 2013: The physical science basis* (Vol. 5, pp. 31–33). New York: Cambridge University Press.

Hewitt, B., Lopez, L., Gaibisels, K., Murdoch, A., Higgins, S., Magnuson, J., et al. (2018). Historical trends, drivers, and future projections of ice phenology in small north temperate lakes in the Laurentian Great Lakes region. *Watermark*, 10(1). <https://doi.org/10.3390/w10010070>

Kang, S., Xu, Y., You, Q., Flügel, W.-A., Pepin, N., & Yao, T. (2010). Review of climate and cryospheric change in the Tibetan Plateau. *Environmental Research Letters*, 5(1). <https://doi.org/10.1088/1748-9326/5/1/015101>

Ke, C.-Q., Tao, A.-Q., & Jin, X. (2013). Variability in the ice phenology of Nam Co Lake in central Tibet from scanning multichannel microwave radiometer and special sensor microwave/imager: 1978 to 2013. *Journal of Applied Remote Sensing*, 7. <https://doi.org/10.1117/1.Jrs.7.073477>

Kendall, M. G. (1975). *Rank correlation methods*. London, UK: Griffin.

Kropacek, J., Maussion, F., Chen, F., Hoerz, S., & Hochschild, V. (2013). Analysis of ice phenology of lakes on the Tibetan Plateau from MODIS data. *The Cryosphere*, 7(1), 287–301. <https://doi.org/10.5194/tc-7-287-2013>

Latifovic, R., & Pouliot, D. (2007). Analysis of climate change impacts on lake ice phenology in Canada using the historical satellite data record. *Remote Sensing of Environment*, 106(4), 492–507. <https://doi.org/10.1016/j.rse.2006.09.015>

Liu, Y., Chen, H., Li, H., & Wang, H. (2020). The impact of preceding spring Antarctic oscillation on the variations of lake ice phenology over the Tibetan Plateau. *Journal of Climate*, 33(2), 639–656. <https://doi.org/10.1175/jcli-d-19-0111.1>

Liu, Y., Chen, H. P., Wang, H. J., & Qiu, Y. B. (2018). The impact of the NAO on the delayed break-up date of lake ice over the southern Tibetan Plateau. *Journal of Climate*, 31(22), 9073–9086. <https://doi.org/10.1175/JCLI-D-18-0197.1>

Mann, H. B. (1945). Nonparametric test against trend. *Econometrica*, 13(3), 245–259. <https://doi.org/10.2307/1907187>

Masui, T., Matsumoto, K., Hijioka, Y., Kinoshita, T., Nozawa, T., Ishiwatari, S., et al. (2011). An emission pathway for stabilization at 6 Wm⁻² radiative forcing. *Climatic Change*, 109(1–2), 59–76. <https://doi.org/10.1007/s10584-011-0150-5>

Moss, R. H., Edmonds, J. A., Hibbard, K. A., Manning, M. R., Rose, S. K., van Vuuren, D. P., et al. (2010). The next generation of scenarios for climate change research and assessment. *Nature*, 463(7282), 747–756. <https://doi.org/10.1038/nature08823>

Nagelkerke, N. J. J. B. (1991). A note on a general definition of the coefficient of determination. *Biometrika*, 78(3), 691–692.

O’Reilly, C. M., Sharma, S., Gray, D. K., Hampton, S. E., Read, J. S., Rowley, R. J., et al. (2015). Rapid and highly variable warming of lake surface waters around the globe. *Geophysical Research Letters*, 42, 10,773–710,781. <https://doi.org/10.1002/2015GL066235>

Parry, M., Parry, M. L., Canziani, O., Palutikof, J., Van der Linden, P., & Hanson, C. (2007). *Climate change 2007—Impacts, adaptation and vulnerability: Working group II contribution to the fourth assessment report of the IPCC*. New York: Cambridge University Press.

Pedregosa, F., Varoquaux, G., Gramfort, A., Michel, V., Thirion, B., Grisel, O., et al. (2011). Scikit-learn: Machine learning in Python. *The Journal of Machine Learning Research*, 12(2011), 2825–2830.

Preston, D. L., Caine, N., McKnight, D. M., Williams, M. W., Hell, K., Miller, M. P., et al. (2016). Climate regulates alpine lake ice cover phenology and aquatic ecosystem structure. *Geophysical Research Letters*, 43, 5553–5560. <https://doi.org/10.1002/2016GL069036>

Qiao, B., Zhu, L., & Yang, R. (2019). Temporal-spatial differences in lake water storage changes and their links to climate change throughout the Tibetan Plateau. *Remote Sensing of Environment*, 222, 232–243. <https://doi.org/10.1016/j.rse.2018.12.037>

Qiu, Y., Guo, H., Ruan, Y., Fu, X., Shi, L., & Tian, B. (2017). *A dataset of microwave brightness temperature and freeze-thaw for medium-to-large lakes over the High Asia region (2002–2016)*. Beijing, China: Science Data Bank. <https://doi.org/10.11922/sciencedb.374>

Qiu, Y., Wang, X., Ruan, Y., Xie, P., Zhong, Y., & Yang, S. (2018). Passive microwave remote sensing of lake freeze-thawing over Qinghai-Tibet Plateau. *Journal of Lake Science*, 30(5), 1438–1449. <https://doi.org/10.18307/2018.0525>

Qiu, Y., Xie, P., Leppäranta, M., Wang, X., Lemmetyinen, J., Lin, H., & Shi, L. J. B. E. D. (2019). MODIS-based daily lake ice extent and coverage dataset for Tibetan Plateau. *Big Earth Data*, 3(2), 170–185. <https://doi.org/10.1080/20964471.2019.1631729>

- Riahi, K., Grübler, A., & Nakicenovic, N. (2007). Scenarios of long-term socio-economic and environmental development under climate stabilization. *Technological Forecasting and Social Change*, *74*(7), 887–935. <https://doi.org/10.1016/j.techfore.2006.05.026>
- Riahi, K., Rao, S., Krey, V., Cho, C., Chirkov, V., Fischer, G., et al. (2011). RCP 8.5—A scenario of comparatively high greenhouse gas emissions. *Climatic Change*, *109*(1–2), 33–57. <https://doi.org/10.1007/s10584-011-0149-y>
- Rosenzweig, C., Karoly, D., Vicarelli, M., Neofotis, P., Wu, Q., Casassa, G., et al. (2008). Attributing physical and biological impacts to anthropogenic climate change. *Nature*, *453*(7193), 353–357. <https://doi.org/10.1038/nature06937>
- Sen, P. K. (1968). Estimates of the regression coefficient based on Kendall's tau. *Journal of the American Statistical Association*, *63*(324), 1379–1389. <https://doi.org/10.1080/01621459.1968.10480934>
- Sharma, S., Blagrove, K., Magnuson, J. J., O'Reilly, C. M., Oliver, S., Batt, R. D., et al. (2019). Widespread loss of lake ice around the Northern Hemisphere in a warming world. *Nature Climate Change*, *9*(3), 227–231. <https://doi.org/10.1038/s41558-018-0393-5>
- Sorvari, S., Korhola, A., & Thompson, R. (2002). Lake diatom response to recent Arctic warming in Finnish Lapland. *Global Change Biology*, *8*(2), 171–181. <https://doi.org/10.1046/j.1365-2486.2002.00463.x>
- Thomson, A. M., Calvin, K. V., Smith, S. J., Kyle, G. P., Volke, A., Patel, P., et al. (2011). RCP4.5: A pathway for stabilization of radiative forcing by 2100. *Climatic Change*, *109*(1–2), 77–94. <https://doi.org/10.1007/s10584-011-0151-4>
- van Vuuren, D. P., den Elzen, M. G. J., Lucas, P. L., Eickhout, B., Strengers, B. J., van Ruijven, B., et al. (2007). Stabilizing greenhouse gas concentrations at low levels: An assessment of reduction strategies and costs. *Climatic Change*, *81*(2), 119–159. <https://doi.org/10.1007/s10584-006-9172-9>
- van Vuuren, D. P., Stehfest, E., den Elzen, M. G. J., Kram, T., van Vliet, J., Deetman, S., et al. (2011). RCP2.6: Exploring the possibility to keep global mean temperature increase below 2°C. *Climatic Change*, *109*(1–2), 95–116. <https://doi.org/10.1007/s10584-011-0152-3>
- Wan, W., Long, D., Hong, Y., Ma, Y., Yuan, Y., Xiao, P., et al. (2016). A lake data set for the Tibetan Plateau from the 1960s, 2005 and 2014. *Scientific Data*, *3*(3), 160039. <https://doi.org/10.1038/sdata.2016.39>
- Wan, W., Zhao, L., Xie, H., Liu, B., Li, H., Cui, Y., et al. (2018). Lake surface water temperature change over the Tibetan Plateau from 2001 to 2015: A sensitive indicator of the warming climate. *Geophysical Research Letters*, *45*, 11,177–111,186. <https://doi.org/10.1029/2018GL078601>
- Weber, H., Riffler, M., Noges, T., & Wunderle, S. (2016). Lake ice phenology from AVHRR data for European lakes: An automated two-step extraction method. *Remote Sensing of Environment*, *174*, 329–340. <https://doi.org/10.1016/j.rse.2015.12.014>
- Willmott, C. J. (1982). Some comments on the evaluation of model performance. *Bulletin of the American Meteorological Society*, *63*(11), 1309–1313. [https://doi.org/10.1175/1520-0477\(1982\)063<1309:SCOTEO>2.0.CO;2](https://doi.org/10.1175/1520-0477(1982)063<1309:SCOTEO>2.0.CO;2)
- Wise, M., Calvin, K., Thomson, A., Clarke, L., Bond-Lamberty, B., Sands, R., et al. (2009). Implications of limiting CO₂ concentrations for land use and energy. *Science*, *324*(5931), 1183–1186. <https://doi.org/10.1126/science.1168475>
- Yao, H., Rusak, J. A., Paterson, A. M., Somers, K. M., Mackay, M., Girard, R., et al. (2013). The interplay of local and regional factors in generating temporal changes in the ice phenology of Dickie Lake, south-central Ontario, Canada. *Inland Waters*, *3*(1), 1–14. <https://doi.org/10.5268/iw-3.1.517>
- Yao, T., Thompson, L. G., Mosbrugger, V., Zhang, F., Ma, Y., Luo, T., et al. (2012). Third Pole Environment (TPE). *Environment and Development*, *3*, 52–64. <https://doi.org/10.1016/j.envdev.2012.04.002>
- Yao, X., Li, L., Zhao, J., Sun, M., Li, J., Gong, P., & An, L. (2016). Spatial-temporal variations of lake ice phenology in the Hoh Xil region from 2000 to 2011. *Journal of Geographical Sciences*, *26*, 70–82. <https://doi.org/10.1007/s11442-016-1255-6>
- Yukimoto, S., Adachi, Y., Hosaka, M., Sakami, T., Yoshimura, H., Hirabara, M., et al. (2012). A new global climate model of the Meteorological Research Institute: MRI-CGCM3—Model description and basic performance—. *Journal of the Meteorological Society of Japan. Ser. II*, *90*, 23–64. <https://doi.org/10.2151/jmsj.2012-A02>
- Zhang, G. (2019). *The lakes larger than 1k m² in Tibetan Plateau (V2.0) (1970s–2018)*. Beijing, China: National Tibetan Plateau Data Center. <https://doi.org/10.11888/Hydro.tpd.c.270303>
- Zhang, G., Luo, W., Chen, W., & Zheng, G. (2019). A robust but variable lake expansion on the Tibetan Plateau. *Science Bulletin*, *64*(18), 1306–1309. <https://doi.org/10.1016/j.scib.2019.07.018>
- Zhang, G., Yao, T., Xie, H., Kang, S., & Lei, Y. (2013). Increased mass over the Tibetan Plateau: From lakes or glaciers? *Geophysical Research Letters*, *40*, 2125–2130. <https://doi.org/10.1002/grl.50462>
- Zhang, G., Yao, T., Xie, H., Qin, J., Ye, Q., Dai, Y., & Guo, R. (2014). Estimating surface temperature changes of lakes in the Tibetan Plateau using MODIS LST data. *Journal of Geophysical Research: Atmospheres*, *119*, 8552–8567. <https://doi.org/10.1002/2014JD021615>
- Zhang, G., Yao, T., Xie, H., Zhang, K., & Zhu, F. (2014). Lakes' state and abundance across the Tibetan Plateau. *Chinese Science Bulletin*, *59*, 3010–3021. <https://doi.org/10.1007/s11434-014-0258-x>
- Zhang, H., Qiu, Y., Zheng, Z., Chu, D., & Yang, Y. (2016). Comparative study of the feasibility of cloud removal methods based on MODIS seasonal snow cover data over the Tibetan Plateau. *Journal of Glaciology and Geocryology*, *38*(3), 714–724. <https://doi.org/10.7522/j.issn.1000-0240.2016.0080>